

Electrochemical and Analytical Study of the Corrosion Inhibitory behavior of Expired Pharmaceutical Compounds for C- Steel Corrosion

Ahmad M. El-Desoky¹, Hytham M. Ahmed^{2,*} and Alaa E. Ali³

¹ Engineering Chemistry Department, High Institute of Engineering & Technology (New Damietta), Egypt and Al-Qunfudah Center for Scientific Research (QCSR), Al-Qunfudah University College, Umm Al-Qura University, KSA

² Pharmaceutical Analysis Department, Faculty of Pharmacy, Damanhour University, Damanhour, Egypt

³ Chemistry Department, Faculty of Science, Damanhour University, Damanhour, Egypt,

*E-mail: hmaahmed@yahoo.co.uk

Received: 13 March 2015 / Accepted: 14 April 2015 / Published: 28 April 2015

Expired pharmaceutical compounds cause environmental pollution which can lead to public health problems. Also, they represent economical problems for pharmaceutical companies because of high disposal costs. On the other hand, the widely used corrosion inhibitors have toxicity problems. To solve the above problems, this work aimed to evaluate the effectiveness of selected expired pharmaceutical compounds as corrosion inhibitors. Hydrochlorothiazide (HCT), captopril (CAP) and guaifenesin (GFN) were chosen as representative examples. These drugs were evaluated as corrosion inhibitors for C- steel in 2 M hydrochloric acid solution at 30°C by various analytical techniques. Electrochemical impedance spectroscopy (EIS), potentiodynamic polarization and electrical frequency modulation (EFM) methods were used in this study. Weight loss technique data was also discussed. The electrochemical results indicated that these compounds are efficient inhibitors for C- steel corrosion. Their efficiencies were up to 81.8 % at the tested temperature. The increase in drug concentration caused increase in the corresponding inhibition efficiency (%IE) values. The adsorption amount and the coverage of pharmaceutical molecules were also increased with increasing concentration. The adsorption of these compounds on C- steel surface obeyed the Temkin adsorption isotherm. Polarization curves indicated that, the investigated pharmaceutical compounds were mixed-type inhibitors. The corrosion kinetic parameters were discussed. The chemical data were in good agreement with those obtained from electrochemical methods.

Keywords: chemical techniques, corrosion test, electrochemical techniques, adsorption

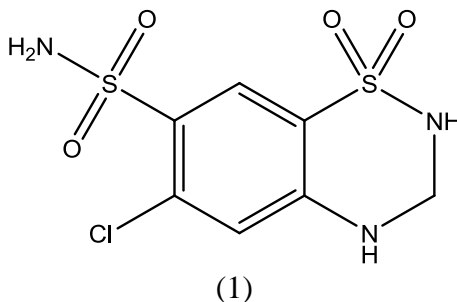
1. INTRODUCTION

Heterocyclic compounds are generally organic compounds containing nitrogen, sulphur and oxygen heteroatoms or which have π electrons in their molecules were proved to be effective inhibitors for metals and their alloys [1-3]. Recently pharmaceutical drugs were used as effective anticorrosion of metals [4, 5]. That was because of their heterocyclic structure [6-8]. These inhibitors adsorbed on the metal surface either physically or chemically[9].

The research performed mainly in the past years identified numerous active drug components that showing inhibitory activity on the corrosion of metals and alloys [10, 11]. In a recent review[8], seventeen drug categories has been presented as corrosion inhibitors for different metals and alloys, in various corrosive media [8]. Most of the pharmaceutical compounds are much more expensive than organic corrosion inhibitors. Moreover, the existence of unused drugs in the environment is harmful to humans [12-17]. On the other hand, deactivation of these drugs is generally carried out with the risk of air pollution with toxic compounds containing N, S, P or halogen atoms. In most cases expired drugs can be tested as corrosion inhibitors, whereas the active substance degrades only infinitesimally. FDA proved that 90% of the drugs are stable for long time after the expiration dates[1]. On the other side, the widely used corrosion inhibitors are toxic and there are environmental regulations which control their usage and disposal [8]. Therefore, this study was focused on inhibitory properties of expired drugs by using analytical techniques. This type of analytical chemistry research can solve two major environmental and economical problems: limitation of environmental pollution with pharmaceutically compounds and reduction of the disposal costs of expired drugs. Moreover, this research would give effective non-hazardous alternatives to toxic corrosion inhibitors.

C-steel was chosen in this study to be the metal under investigation. It chemically contains of C, Cr, Ni, Si, Mn, P, S and Fe with 0.14, 0.1, 0.01, 0.24, 0.5, 0.05, 0.05 and 98.91 weight % respectively. C- steel is so important in petroleum industries [18]. This type of steels is relatively low corrosion resistance in acidic solution [19-23]. Therefore, several corrosion inhibition methods used to minimize C- steel corrosion. Organic inhibitors were used in such purpose [24-30].

In this work selected pharmaceutical compounds [31-33] (Figure 1); Hydrochlorothiazide (HCT) 6-Chloro-1,1-dioxo-3,4-dihydro-2H-1,2,4-benzothiadiazine-7-sulfonamide, Captopril (CAP), 1-((s)-3-mercapto-2-methyl propanoyl) pyrrolidine-2-carboxylic acid and Guaifenesin (GUA), 3-(2-methoxy phenoxy) propane 1,2-diol were tested for the first time as C-steel corrosion inhibitors. Therefore, the inhibition characteristics of HCT,CAP and GUA were investigated as corrosion inhibitors for C- steel in 2 M HCl solution using chemical and electrochemical techniques. The inhibition mechanism has been discussed on the basis of these studies.



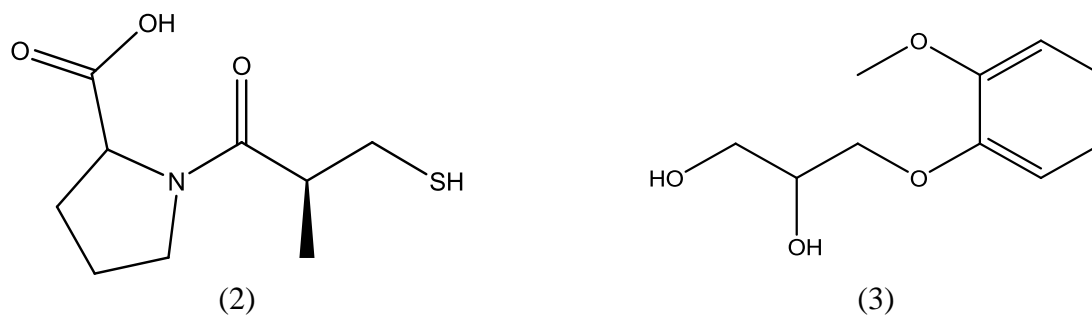


Figure 1. Chemical structures of (1) hydrochlorothiazide, (2) captopril and (3) Guaifenesin.

In this work selected pharmaceutical compounds [31-33] (Figure 1); Hydrochlorothiazide (HCT) 6-Chloro-1,1-dioxo-3,4-dihydro-2H-1,2,4-benzothiadiazine-7-sulfonamide, Captopril (CAP), 1-((S)-3-mercapto-2-methyl propanoyl) pyrrolidine-2-carboxylic acid and Guaifenesin (GUA), 3-(2-methoxy phenoxy) propane 1,2-diol were tested for the first time as C-steel corrosion inhibitors. Therefore, the inhibition characteristics of HCT, CAP and GUA were investigated as corrosion inhibitors for C- steel in 2 M HCl solution using chemical and electrochemical techniques. The inhibition mechanism has been discussed on the basis of these studies.

2. EXPERIMENTAL

2.1. Chemicals and materials

Hydrochloric acid (37 %), ethanol and acetone were purchased from Al-gomhoria Company. Deionized distilled water was used in all performed experiments.

2.2. Analytical Methods

2.2.1. Weight loss measurements

C- steel specimens (2.1 x 2.0 x 0.2 cm) were abraded with different grades of emery paper, degreased with acetone, rinsed with double distilled water then dried using filter papers. After accurate weighting, the specimens were transferred to conical flask. Then 100 ml of 2 M HCl were added to immerse the specimens. This experiment was done in the absence and presence various concentrations of inhibitors at 30 °C. Effect of variety immersion time (0.5- 3 hrs) was tested. After each period of time C- steel samples were taken out then washed with double distilled water. After that dried and weighted. Weight loss data were used to calculate the rate of corrosion (R) in mmy^{-1} by Eq. (1):

$$R = (\text{weight loss in gram} \times 8.75 \times 10^4) / DAT \quad (1)$$

where D is C- steel density in g cm^{-3} , A is area of exposure (cm^2), T is time of exposure (hr).

The inhibition efficiency (%IE) and coverage degree of the surface (θ) were calculated by Eq. (2):

$$\%IE = \theta \times 100 = [(R^* - R) / R^*] \times 100 \quad (2)$$

where R and R^* are the rates of corrosion of C- steel in presence and absence of inhibitor, respectively.

2.2.2. Electrochemical measurements

Gamry potentiostat/galvanostat/ZRA (model PCI300/4) was used for electrochemical measurements, EIS and EFM. In these measurements, platinum foil and saturated calomel electrode (SCE) were used as counter and reference electrodes, respectively. The C- steel electrodes were 1x1 cm and were welded from one side to a copper wire used for electrical connection. The electrodes were abraded, degreased and rinsed as described above. Temperature was $(30 \pm 1^\circ\text{C})$ in all experiments. Curves of potentiodynamic were observed in range from -500 to 500 mV at a scan rate 1 mV S^{-1} after the steady state is reached (0.5 hr) and the open circuit potential (OCP) was noted. The % IE and coverage degree of the surface were calculated by Eq. (3):

$$IE\% = \theta \times 100 = [1 - (i_{\text{corr}}^0 / i_{\text{corr}})] \times 100 \quad (3)$$

where i_{corr}^0 and i_{corr} are densities of corrosion current of inhibited and uninhibited solutions, respectively.

EIS and EFM data were collected through ESA400. Gamry applications include software EIS300 and EFM140 were used for EIS and EFM measurements respectively. Data were collected by computer. The obtained data were plotted, graphed and fitted by using Echem Analyst 5.5 Software. EIS experiments were carried out with amplitude of 5 mV peak-to-peak in a frequency range of 100 kHz to 10 mHz using ac signals at respective corrosion potential. EFM carried out using two frequencies 2 and 5 Hz with amplitude of 10 mV. The frequency base was 1 Hz.

2.2.3. Theoretical study

Quantum chemical calculations were done by using Accelrys (Material Studio Version 4.4) software.

3. RESULTS AND DISCUSSION

3.1. Weight loss measurements

Inhibition effect of HCT different concentrations on C- steel corrosion in 2 M HCl was examined by weight loss method. Weight loss–time curves in the presence and absence of HCT were as shown in figure (2). As shown in table (1), the %IE values were directly proportional to inhibitor concentration (3×10^{-5} to 15×10^{-5} M). The highest %IE value was achieved at 15×10^{-5} M. The lowest %IE is obtained in the presence of GFN, therefore %IE values decreased in the following order: HCT > CAP > GFN.

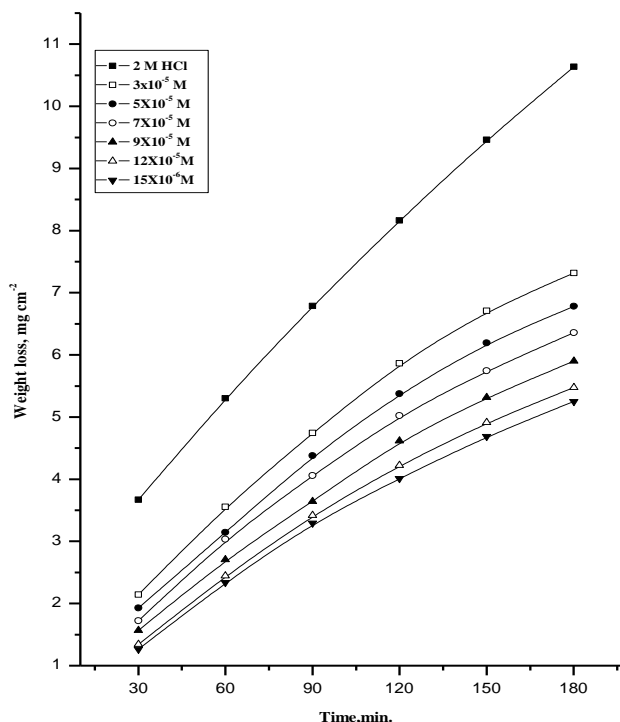


Figure 2. Weight loss-time curves for C- steel dissolution in 2 M HCl in the absence and presence of different concentrations of inhibitor (I) at 30 °C.

Table 1. % IE values of C- steel after 2hrs immersion period of time in 2 M HCl in presence of various concentrations of tested pharmaceutical compounds at 30 °C.

Conc.,x10 ⁻⁵ M	% IE		
	HCT	CAP	GFN
3	68.9	61.7	57.3
5	71.1	66.3	59.9
7	75.0	68.7	64.2
9	77.6	71.8	66.1
12	78.8	74.8	67.6
15	81.8	77.9	71.4

3.1.1. Adsorption isotherm

Assuming the corrosion inhibition was caused by the adsorption of the examined pharmaceutical compounds, and the values of surface coverage for different concentrations of pharmaceutical compounds in 2 M HCl were evaluated from weight loss. It was observed that, θ values increased with increasing the concentration of the tested pharmaceutical compounds. Using these surface coverage values, different adsorption isotherms could be applied to the obtained experimental data. The Temkin adsorption isotherm was used to suggest the mechanism of adsorption, by plotting (θ) vs. $\log C$, and straight lines were obtained Figure (3). Adsorption process parameters for that were obtained as shown in Table (2).

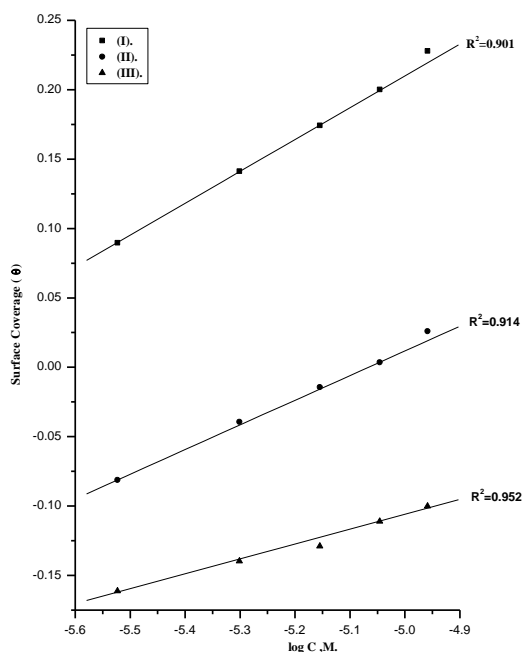


Figure 3. Temkin adsorption isotherm for obtained C- steel corrosion data in 2 M HCl at 30°C in the presence of different drugs concentrations. [I: HCT, II: CAP and III: GFN]

Table 2. Inhibitor equilibrium constant (K), free energy of adsorption (ΔG°_{ads}), and the interaction parameter (a) for pharmaceutical compounds at 30°C.

Inhibitors	Temkin model		
	a	K, M ⁻¹	- ΔG°_{ads} , kJ mol ⁻¹
HCT	13.9	72.8	63.0
CAP	13.7	67.8	59.2
GFN	13.4	17.0	51.8

Free energy of adsorption ΔG°_{ads} values were negative and increased along with the % IE increase. This indicated that the tested pharmaceutical compounds were strongly adsorbed on C- steel surface and showed the spontaneity of the adsorption process and stability of the adsorbed layer on the C- steel surface. Generally, ΔG°_{ads} values up to -20 kJmol⁻¹ are consistent with the electrostatic interaction between the charged molecules and the charged metal which confirmed physical adsorption. On the other hand, ΔG°_{ads} values which were more negative than -40 kJ mol⁻¹ indicated that the inhibitor molecules share or transfer electrons to the surface of the metal forming a coordinate bond which indicated chemisorptions [34]. The values of ΔG°_{ads} obtained were approximately equal to -52 ± 1 kJ mol⁻¹, indicated that the adsorption mechanism of the investigated pharmaceutical compounds on C- steel in 2 M HCl solution involved chemisorptions [35].

3.1.2. Effect of temperature

The activation energies (E_a^*) for the C- steel corrosion in the absence and presence of different concentrations of the examined drugs were calculated using Arrhenius-type Eq 4 [36]:

$$\log k = \log A - E_a^* / 2.303RT \tag{4}$$

where A is the pre-exponential factor, k is the rate constant, E_a^* is the apparent activation energy of the corrosion process, R is the universal gas constant and T is the absolute temperature. Arrhenius plots of log k vs. 1/T for C- steel in 2 M HCl in the absence and presence of different concentration of HCT are shown graphically in figure (4).

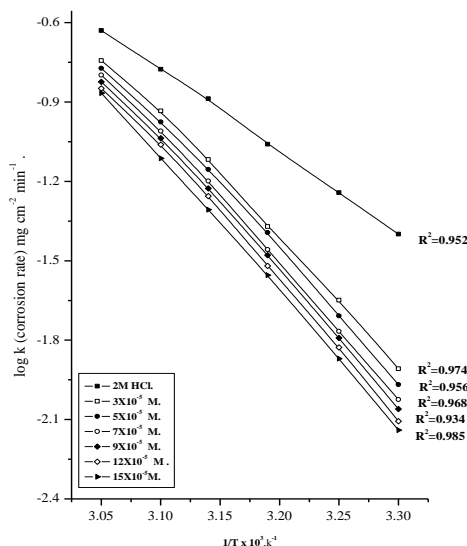


Figure 4. log k (corrosion rate) - 1/T curves for C- steel dissolution in 2 M HCl in the absence and presence of various HCT concentrations.

The variation of logk vs. 1/T is a linear one and E_a^* values were calculated from the slope of these lines and given in Table (3).

The increase in E_a^* values along with the increase of tested compounds concentrations indicated that, the energy barrier for the corrosion reaction increased. Moreover, It indicated also that the whole process was controlled by surface reaction, since the activation energy of the corrosion process was larger than 20 kJmol⁻¹ [37].

Enthalpy and entropy of activation (ΔH^* , ΔS^*) for the corrosion of C- steel in 2 M HCl were obtained by applying the transition state Eq(5) :

$$k = (RT/ Nh) \exp (\Delta S^*/R) \exp (-\Delta H^*/RT) \tag{5}$$

where h is Planck’s constant, N is Avogadro’s number. A plot of log k/T vs 1/T also gave straight lines as shown in Figure (5) for C- steel dissolution in 2 M HCl in the absence and presence of different concentration of HCT. Slopes of these lines equal $-\Delta H^*/2.303R$ and the intercept equal $\log RT/Nh + (\Delta S^*/2.303R)$ from which the value of ΔH^* and ΔS^* were calculated and tabulated in Table(3). According to these results, it was clear that the presence of the tested compounds increased the activation energy values and hence decreased the corrosion rate of the C- steel. These results also

indicated that these tested compounds acted as inhibitors through increasing activation energy of C- steel dissolution by making a barrier to mass and charge transfer by their adsorption on C- steel surface. Positive sign of the enthalpies reflected the endothermic nature of the steel dissolution process.

Table 3. Activation parameters for C-steel dissolution in the presence and absence of various concentrations of drugs in 2 M HCl at 30 °C.

Inhibitor	Conc., $\times 10^{-5}$ M.	Activation parameters		
		E_a^*	ΔH_a^*	$-\Delta S_a^*$
		kJ mol^{-1}	kJ mol^{-1}	$\text{J mol}^{-1} \text{K}^{-1}$
Free Acid (2 M HCl)	0	46.5	45.2	42.3
HCT	3	49.0	47.4	35.3
	5	51.6	50.0	31.2
	7	52.9	52.2	26.9
	9	55.3	53.6	21.7
	12	57.5	54.5	17.1
	15	60.7	56.6	14.7
CAP	3	47.9	46.0	37.2
	5	49.5	48.1	33.1
	7	50.9	49.6	29.5
	9	53.6	51.3	27.4
	12	54.2	52.6	22.9
	15	57.3	54.0	22.7
GFN	3	46.5	44.6	38.1
	5	47.2	47.4	33.7
	7	49.1	48.2	30.1
	9	50.5	49.6	28.5
	12	51.9	50.1	24.3
	15	53.5	52.0	23.3

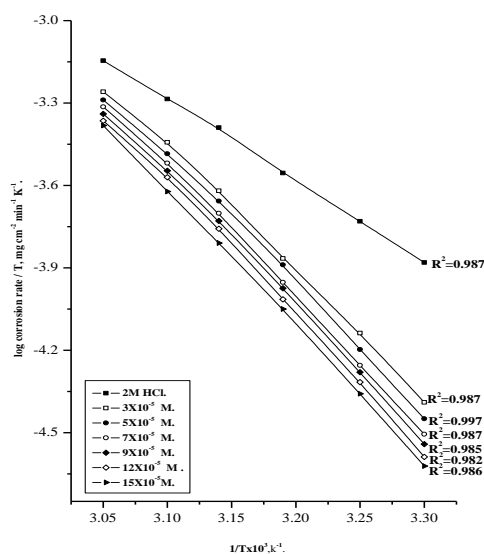


Figure 5. log (corrosion rate/T) - (1/T) curves for C- steel dissolution in 2 M HCl in the absence and presence of various HCT concentrations.

All values of E_a^* were larger than the corresponding ΔH_a^* values indicating that the corrosion process must involved a gaseous reaction, simply the hydrogen evolution reaction, associated with a decrease in the total reaction volume [38].

The ΔS^* values were large and negative in presence and absence of the examined drugs; this indicated that the activated complex in the rate-determining step represented an association rather than dissociation step, meaning that a decrease in disordering took place on going from reactants to the activated complex [39, 40].

3.2. Potentiodynamic polarization studies

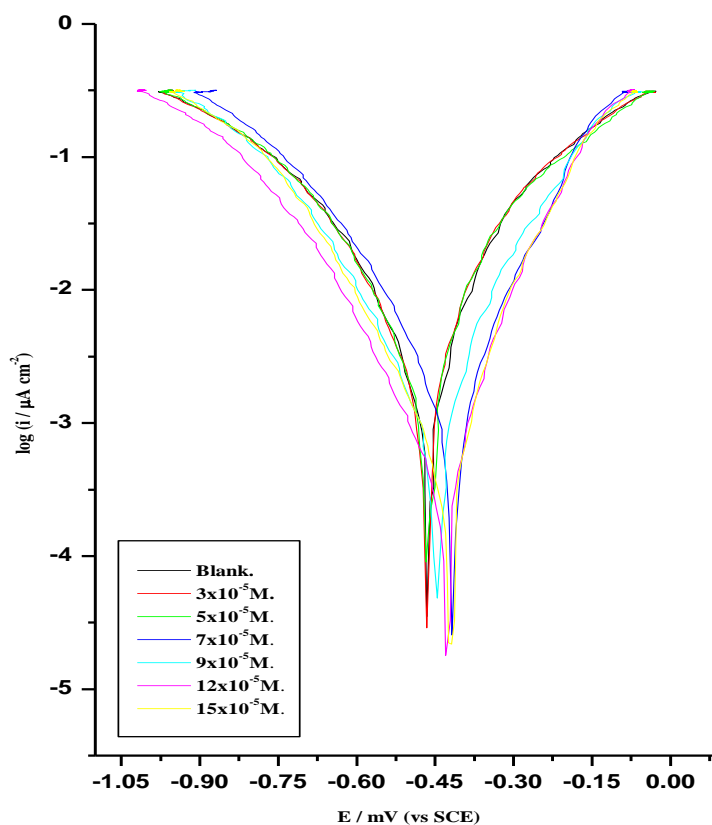


Figure 6. Potentiodynamic polarization curves for C- steel in 2 M HCl at 30°C [in the presence and absence of various HCT concentrations].

The cathodic and anodic polarization curves of C- steel in 2 M HCl solution in presence and absence of various concentrations of the HCT at 30 °C are shown in figure (6). The different electrochemical parameters were obtained by using Tafel plots as shown in table (4).

In presence of the examined compounds, a low corrosion current density (i_{corr}) values were observed without significant changes in corrosion potential (E_{corr}). This indicated that the investigated compounds were mixed type inhibitors. Moreover, that indicated that, these inhibitors were adsorbed on the surface leading to block the corrosion reaction [41]. Also, the data showed that the anodic and

the cathodic Tafel slopes (β_a and β_c) were slightly changed on the increase of the tested compounds concentration. This indicated that there was no change in the inhibition mechanism in presence and absence of drugs. The β_c values were slightly higher than the β_a values which indicated a cathodic action of the inhibitor. The Tafel slope high values can be attributed to surface kinetic process rather the diffusion-controlled process [42].

Table 4. Effect of concentrations of the investigated pharmaceutical compounds on E_{corr} , i_{corr} , β_a , β_c , θ and % IE for C-steel corrosion in 2M HCl at 30°C.

Concentration, $\times 10^{-5}\text{M}$		$-E_{\text{corr}}$, mV	i_{corr} , mA cm^{-2}	β_c , mV dec^{-1}	β_a , mV dec^{-1}	θ	% IE
2M HCl		466.7	0.0820	311.1	282.7	-	-
HCT	3	467.4	0.0318	207.1	174.7	0.612	61.2
	5	460.3	0.0317	216.5	179.6	0.613	61.3
	7	411.8	0.0307	182.5	124.1	0.625	62.5
	9	452.1	0.0266	173.1	193.3	0.675	67.5
	12	448.9	0.0220	144.4	119.2	0.731	73.1
	15	427.6	0.0217	147.3	105.4	0.735	73.5
CAP	3	465.7	0.0452	265.6	228.3	0.448	44.8
	5	464.7	0.0391	257.2	219.5	0.523	52.3
	7	416.6	0.0379	209.5	147.4	0.537	53.7
	9	447.6	0.0354	210.5	162.7	0.568	56.8
	12	428.3	0.0296	209.3	129.7	0.639	63.9
	15	421.6	0.0283	182.4	126.3	0.654	65.4
GFN	3	463.7	0.0651	293.5	259.2	0.206	20.6
	5	469.1	0.0626	248.3	227.9	0.236	23.6
	7	455.2	0.0490	232.5	189.5	0.402	40.2
	9	457.3	0.0377	221.3	188.2	0.540	54.0
	12	450.0	0.0322	204.6	167.7	0.607	60.7
	15	415.2	0.0318	204.3	146.8	0.612	61.2

3.3. Electrochemical impedance spectroscopy (EIS)

The EIS provided valuable information which is mechanistic and kinetic for an electrochemical system under examination. The observed Nyquist impedance plots of C- steel electrode at respective corrosion potentials after immersion period (0.5 hr) in 2M HCl in absence and presence of different

HCT concentrations as shown in Figure (7). This figure exhibited a single semi-circle shifted along the real impedance (Z_r).

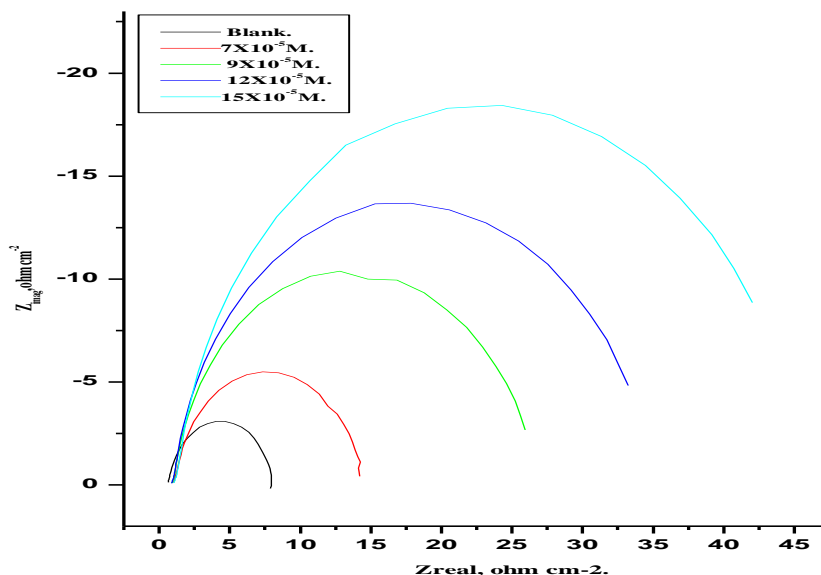


Figure 7. The Nyquist plots for C- steel in 2 M HCl solution in the absence and presence of different concentrations of HCT at 30°C.

From the theory of EIS, HCT was expected to give excellent semicircles through the Nyquist plots. However, the impedance loops measurements were depressed semi-circles and their centers were below the real axis. This phenomenon was known as the “dispersing effect” due to frequency dispersion [43] and mass transport resistant [6] and electrode surface heterogeneity due to surface roughness, impurities, dislocations, grain boundaries, adsorption of inhibitors, formation of porous layers [44-46], etc. so one constant phase element (CPE) was substituted for the capacitive element, to explain the depression of the capacitance semi-circle, to give a more accurate fit. Impedance data were analyzed using the circuit as shown in Figure (8); in which R_s and R_{ct} represented the electrolyte and the charge-transfer resistances respectively and CPE. The correction of capacity to its real values was obtained by using Eq. (6)[46]:

$$C_{dl} = Y_o (\omega_{max})^{n-1} \tag{6}$$

where Y_o is the CPE coefficient, ω_{max} is the frequency at which the imaginary part of impedance ($-Z_i$) has a maximum and n is the CPE exponent (phase shift).

Table (7) showed the obtained data from fitted spectra. The %IE was calculated from Eq. (7):

$$\%IE = \left(1 - \frac{R_{ct}^o}{R_{ct}} \right) \times 100 \tag{7}$$

where R_{ct} and R_{ct}^* are the charge-transfer resistances in the absence and presence of the used drugs, respectively.

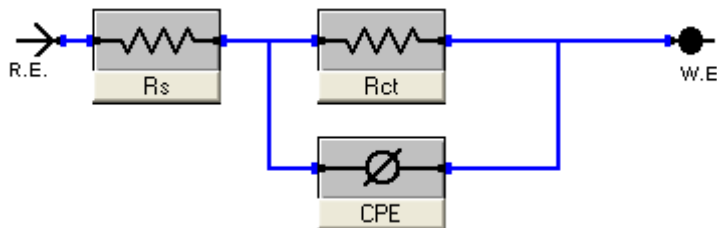


Figure 8. The equivalent circuit model used to fit the experimental results

Table 5. EIS obtained data for electrochemical kinetic parameters for the corrosion of C-steel in 2 M HCl at 30 °C with various concentrations of tested compounds.

compounds	Drug Concentration, $\times 10^{-5}M$	$C_{dl}, \mu F cm^{-2}$	$R_{ct}, ohm cm^2$	θ	%IE
Blank	2 M HCl	119.3	6.89	0.000	0.0
HCT	7	108.8	13.97	0.506	50.6
	9	104.6	24.62	0.719	71.9
	12	103.7	34.52	0.800	80.0
	15	96.8	41.03	0.831	83.1
CAP	7	107.0	13.13	0.474	47.4
	9	103.7	22.32	0.691	69.1
	12	102.2	28.83	0.760	76.0
	15	96.1	37.83	0.817	81.7
GFN	7	106.8	12.96	0.468	46.8
	9	102.1	21.49	0.679	67.9
	12	101.7	27.62	0.750	75.0
	15	95.9	35.09	0.803	80.3

Data in Table (5) showed that; the obtained R_s values were much smaller than R_{ct} values. Also; R_{ct} values increased and the calculated C_{dl} values decreased with the increase of the inhibitor concentrations, this in turn led to an increase of θ and Y_1 values. High R_{ct} values were generally associated with a slower corroding system [47]. The decrease in the C_{dl} calculated values indicated that inhibitors function by adsorption at the metal/solution interface [48].

The obtained %IE according to EIS data showed a similar attitude as those which came from polarization measurements. The differences in surface status of the electrode in two measurements could be the reason behind the differences of the obtained %IE values from two methods. EIS was set at the rest potential, however to measure polarization, the electrode potential was polarized to high over potential, non-uniform current distributions, produced from cell geometry, solution conductivity,

counter and reference electrode placement, etc., would cause variation between the area of the electrode where polarization occurred and the total area [49].

3.4. Electrochemical Frequency Modulation (EFM)

Table 6. EFM data for electrochemical kinetic parameters for the corrosion of C- steel in 2 M HCl at 30°C with different concentrations pharmaceutical compounds.

Inhibitor	Conc. $\times 10^{-5}$ M	$i_{\text{corr.}}$, $\mu\text{A cm}^{-2}$	β_a , mV dec^{-1}	β_c , mV dec^{-1}	CF-2	CF-3	IE %
Blank	0.0	463.5	143	217	1.9	3.1	-----
HCT	7	244.3	109	136	2.0	3.2	47.2
	9	200.0	104	138	1.8	2.9	56.8
	12	146.0	147	157	1.9	2.9	68.5
	15	119.2	138	164	2.0	3.3	74.2
CAP	7	249.6	121	147	2.1	2.8	46.1
	9	211.2	114	135	2.0	2.7	54.4
	12	158.3	165	169	2.2	2.8	65.8
	15	141.4	151	154	2.0	2.7	69.4
GFN	7	327.2	111	139	2.1	3.1	29.4
	9	245.0	139	153	2.2	3.0	47.1
	12	207.4	118	127	2.3	3.2	55.2
	15	210.4	110	126	2.0	3.0	54.6

EFM was recently proposed as a new electrochemical method for online corrosion monitoring [47, 50-52]. EFM is a rapid and nondestructive corrosion rate measurement technique which gives corrosion current values with no need to Tafel constants.

It is well known that the corrosion process is non-linear in nature. EFM can use this non-linear response in the corrosion current calculation via the available information about the corroding system. EFM data can be shown in Figure (9), the current response includes both the input frequencies and frequency components which are the sum, difference, and multiples of the two input frequencies.

The electrochemical corrosion kinetic parameters at different concentrations of investigated pharmaceutical compounds in 2 M HCl at 30°C were shown in Table (6). The %IE values were found to increase with the increase in the inhibitors concentrations. The causality factors CF-2 and CF-3 in Table (6) were around their theoretical values of 2.0 and 3.0, respectively. Therefore, the obtained data were of good quality. The calculated %IE values which derived from weight loss, Tafel polarization and EIS measurements were in good agreement with those obtained from EFM measurements.

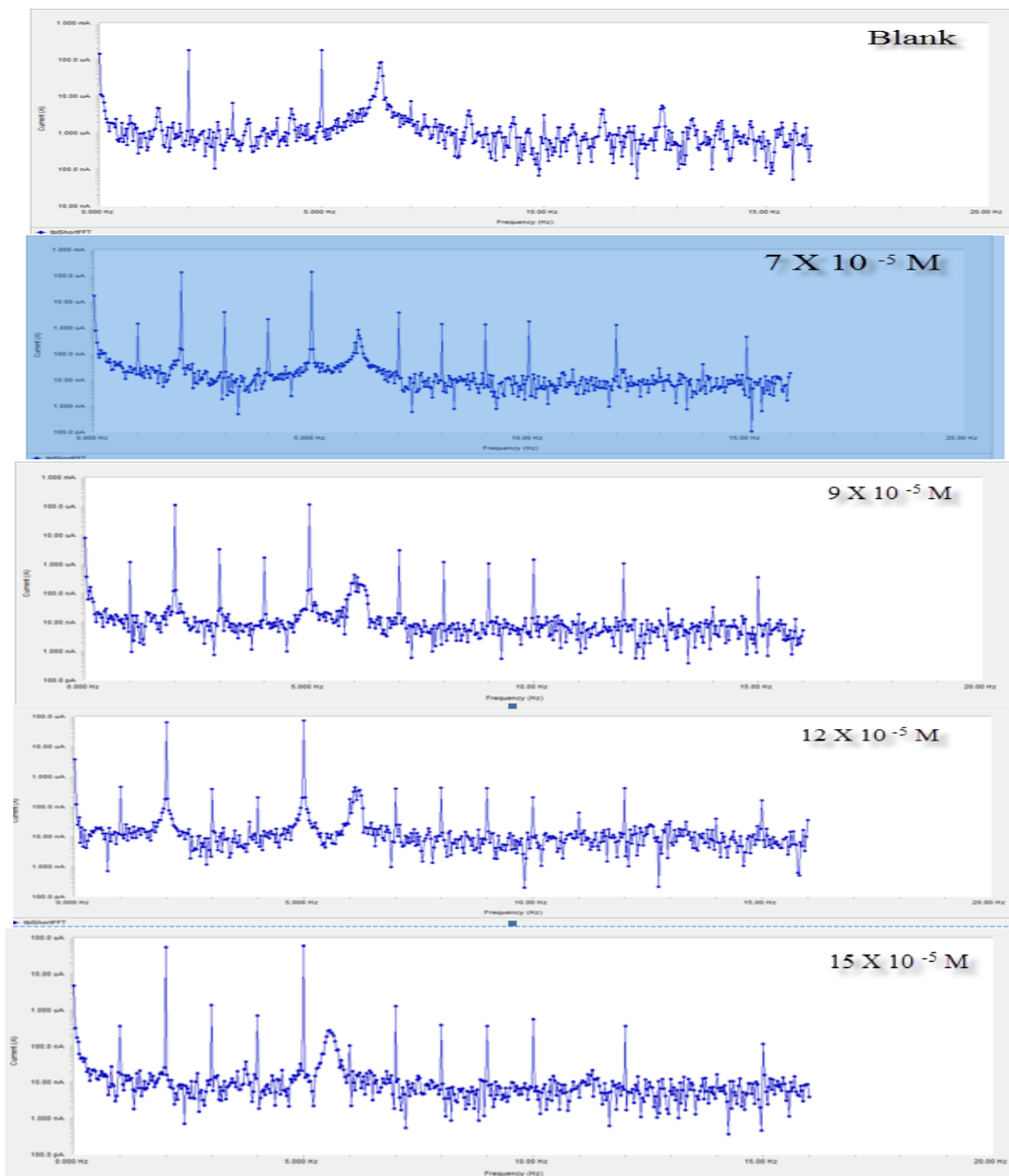


Figure 9. Electrochemical kinetic parameters obtained from EFM technique for the corrosion of C-steel in 2 M HCl at different concentrations of pharmaceutical compounds at 30°C.

3.5. Computational study

Quantum-chemical calculations have proved to be used for studying corrosion inhibition mechanism [53]. There are some quantum chemical parameters which could be related to the metal-inhibitor interactions. One of these parameters is the energy of the HOMO which is correlated to the capacity of a molecule to give electrons. So, an increase of E_{HOMO} value can facilitate the adsorption and therefore the %IE, by indicating the disposition of the molecule to donate orbital electrons to an appropriate acceptor with empty molecular orbital. In the same way low values of energy gap

difference $\Delta E = E_{\text{LUMO}} - E_{\text{HOMO}}$ (the energy required to move an electron from HOMO to LUMO) would render good inhibition efficiencies, because the required energy to remove an electron from the last occupied orbital will be low [54]. Also, low dipole moment μ values would favor the accumulation of inhibitor molecules on metallic surface [55].

Table 7. The calculated quantum chemical parameters of the investigated pharmaceutical compounds

	HCT	CAP	GFN
$-E_{\text{HOMO}}$ (eV)	9.114	9.342	9.368
$-E_{\text{LUMO}}$ (eV)	1.056	0.126	0.110
ΔE (eV)	8.058	9.216	9.276
η (eV)	4.029	4.608	4.629
σ (eV ⁻¹)	0.248	0.214	0.216
$-\pi$ (eV)	5.085	4.734	4.739
χ (eV)	5.085	4.734	4.739

The Mulliken charge densities of investigated compounds have been calculated together with some physical characters like the E_{HOMO} , E_{LUMO} , $\Delta E = E_{\text{LUMO}} - E_{\text{HOMO}}$ and dipole moment (μ) (Table 7). The results suggested that both the gap energy ΔE value, as well as the dipole moment μ value, favor HCT, indicating its effectiveness as a corrosion inhibitor.

The reactive ability of the inhibitor was related to E_{HOMO} and E_{LUMO} [56]. Higher E_{HOMO} of the adsorbent increased electron donating ability [57]. Low E_{LUMO} indicated that the acceptor gained electrons easily. The obtained quantum chemical indices (E_{HOMO} , E_{LUMO} , μ) of examined drugs are shown in Table (7). Low ΔE enables adsorption of the molecule and raise %IE.

The bond gap energy ΔE increased from HCT to GFN. These results clarify the decreasing %IE in this order HCT > CAP > GFN, as shown in Table (7). Therefore, the estimated energy gaps showed reasonably good correlation with the efficiency of corrosion inhibition. Furthermore, according to data shown in Table (7), it was indicated that HCT possesses the lowest total energy which means that HCT adsorption occurs easily and was favored by the highest softness.

3.6. Corrosion inhibition mechanism

Inhibition of the corrosion of C- steel in 2 M HCl solution by investigated pharmaceutical compounds was determined by weight loss, potentiodynamic polarization measurements, EIS, and EFM methods, it was found that the %IE depended on concentration, nature of metal, the mode of adsorption of the inhibitors and surface conditions.

The adsorption of inhibitor depended on its concentration. At adsorption density less than a monolayer, most of the nucleation sites were still possibly exposed to HCl, since inhibitor adsorbed

less likely on them. When the adsorption density reached monolayer adsorption, some of the nucleation sites began to be covered by inhibitor molecules. At maximum adsorption density, the inhibitor molecules covered the whole surface, including the nucleation sites, and then complete inhibition occurred.

The obtained corrosion data in the presence of the investigated compounds can be described as follows; the corrosion rate and current decreased with the increase of these compounds concentration. Also, there was a linear variation of weight loss with time. Moreover, Tafel lines were shifted to higher potential regions. Furthermore, corrosion inhibition decreased with the increase of temperature indicated desorption of the adsorbed inhibitor molecules occurred. Finally, the %IE relayed on the number of adsorption active centers in the molecule and their charge densities.

In this work, C-steel corrosion inhibition suggested to be attributed to adsorption of the inhibitors at the electrode/ solution interface, the extent of adsorption of an inhibitor depended on the nature of the metal, the mode of adsorption of the inhibitor and the surface conditions. Adsorption on C-steel surface was suggested to be via the active centers attached to the tested drugs and rely on their charge density. Nitrogen atoms donate lone pairs of electrons to the C-steel surface forming coordinate bond.

The mode of adsorption depended on the affinity of the metal towards the π -electron clouds of the ring system. The order of decreasing the %IE of the tested drugs in the corrosive solution was as follows: HCT > CAP > GFN

HCT exhibited perfect inhibition power due to it has the largest molecular weight (297.74) which means largest size. This might facilitate biggest surface coverage. Also, HCT adsorbed through nine active adsorption centers in its chemical structure which are four oxygen, two sulphur and three nitrogen atoms. Moreover, the sharing of three valence lone pairs of electrons of the chloride atom with phenyl group enabled it to be a donor by mesomeric effect and increase the electron density on HCT. CAP came after HCT in %IE, because it had lesser molecular weight (217.29). Also, it has only five active centers, which are one sulphur, one nitrogen and three oxygen, atoms. GFN was the weakest as it has the lowest %IE. This could be attributed to it has the lowest molecular size (198.22) and lowest number of adsorption centers which are only four oxygen atoms.

4. CONCLUSIONS

The investigated pharmaceutical compounds HCT, CAP, and GFN inhibited the corrosion of C- steel in 2 M HCl. The inhibition was attributed to adsorption of these compounds on the C- steel surface via the blockage of its active sites. The adsorption of pharmaceutical compounds fitted Temkin isotherm. The obtained data of weight loss, DC polarization, and AC impedance techniques were in good agreement. All data indicated that the %IE increased along with the increase of inhibitor concentration. The investigated compounds acted as mixed-type inhibitor in 2 M HCl as indicated by the polarization data. EIS data indicated that an increase in the charge transfer resistance and a decrease in double layer capacitances when the inhibitor added and hence an increase in % IE. This was attributed to the increase of the electrical double layer thickness. The order of % IE of these

investigated compounds was in the following order: HCT > CAP > GFN. Finally, E_{HOMO} and E_{LUMO} values decreased along with the increase in % IE obtained values.

References

1. N. Vaszilcsin, V. Ordodi, A. Borza, *Int. J. Pharm.* 431 241-244.
2. M.A. Khalifa, M. El-Batouti, F. Mahgoub, A.B. Aknish, *Materials and Corrosion-Werkstoffe Und Korrosion* 54 (2003) 251-258.
3. Y. Abboud, A. Abourriche, T. Saffaj, M. Berrada, M. Charrouf, A. Bennamara, N. Al Himidi, H. Hannache, *Materials chemistry and physics* 105 (2007) 1-5.
4. I. Naqvi, A.R. Saleemi, S. Naveed, *International Journal of Electrochemical Science* 6 (2011) 146-161.
5. M. Abdallah, I. Zaafarany, S.O. Al-Karane, A.A. Abd El-Fattah, *Arabian Journal of Chemistry* 5 (2012) 225-234.
6. K.F. Khaled, *Electrochimica Acta* 48 (2003) 2493-2503.
7. A. Popova, M. Christov, S. Raicheva, E. Sokolova, *Corrosion Science* 46 (2004) 1333-1350.
8. G. Gece, *Corrosion Science* 53 (2011) 3873-3898.
9. E. McCafferty, *Introduction to corrosion science*, Springer Science & Business Media, 2010.
10. M. Abdallah, *Corrosion Science* 46 (2004) 1981-1996.
11. T. Arslan, F. Kandemirli, E.E. Ebenso, I. Love, H. Alemu, *Corrosion Science* 51 (2009) 35-47.
12. I.S. Ruhoy, C.G. Daughton, *Science of the Total Environment* 388 (2007) 137-148.
13. M.A. Patwary, W.T. O'Hare, M.H. Sarker, *Safety Science* 49 (2011) 1200-1207.
14. [M. Kotchen, J. Kallaos, K. Wheeler, C. Wong, M. Zahller, *Journal of Environmental Management* 90 (2009) 1476-1482.
15. J. Feitosa-Felizzola, S. Chiron, *Journal of Hydrology* 364 (2009) 50-57.
16. J.P. Bound, N. Voulvoulis, *Water Research* 40 (2006) 2885-2892.
17. S.K. Khetan, T.J. Collins, *Chemical Reviews* 107 (2007) 2319-2364.
18. M.A. Deyab, *Corrosion Science* 49 (2007) 2315-2328.
19. S.A.A. El-Maksoud, A.S. Fouda, *Materials chemistry and physics* 93 (2005) 84-90.
20. K.F. Khaled, *Materials chemistry and physics* 112 (2008) 290-300.
21. E. Machnikova, K.H. Whitmire, N. Hackerman, *Electrochimica Acta* 53 (2008) 6024-6032.
22. H. Ashassi-Sorkhabi, M.R. Majidi, K. Seyyedi, *Applied surface science* 225 (2004) 176-185.
23. M.A. Migahed, I.F. Nassar, *Electrochimica Acta* 53 (2008) 2877-2882.
24. G.I. Avci, *Colloids and Surfaces A: Physicochemical and Engineering Aspects* 317 (2008) 730-736.
25. A.B. Tadros, B.A. Abdelnabey, *Journal of Electroanalytical Chemistry* 246 (1988) 433-439.
26. J.O. Bockris, Y. Bo, *Journal of the Electrochemical Society* 138 (1991) 2237-2252.
27. M. Abdallah, E.A. Helal, A.S. Fouda, *Corrosion Science* 48 (2006) 1639-1654.
28. A.S. Fouda, A.A. Al-Sarawy, E.E. El-Katori, *Chemical Papers-Chemicke Zvesti* 60 (2006) 5-9.
29. A.S. Fouda, A.A. Al-Sarawy, E.E. El-Katori, *Desalination* 201 (2006) 1-13.
30. O. Benali, L. Larabi, M. Traisnel, L. Gengembre, Y. Harek, *Applied surface science* 253 (2007) 6130-6139.
31. R.C. Heel, R.N. Brogden, T.M. Speight, G.S. Avery, *Drugs* 20 (1980) 409-452.
32. K. Wellington, D.M. Faulds, *Drugs* 62 (2002) 1983-2005.
33. R.S. Irwin, M.J. Rosen, S.S. Braman, *Archives of internal medicine* 137 (1977) 1186-1191.
34. F. Bensajjay, S. Alehyen, M. El Achouri, S. Kertit, *Anti-Corrosion Methods and Materials* 50 (2003) 402-409.
35. S.Z. Duan, Y.L. Tao, *Interface Chem.* Higher Education Press, Beijing 124 (1990).
36. I.N. Putilova, *Metallic corrosion inhibitors*, Pergamon Press, 1960.

37. K.K. Al-Neami, A.K. Mohamed, I.M. Kenawy, A.S. Fouda, *Monatshefte für Chemie/Chemical Monthly* 126 (1995) 369-376.
38. E.A. Noor, *International Journal of Electrochemical Science* 2 (2007) 996-1017.
39. M.B. Smith, J. March, *March's advanced organic chemistry: reactions, mechanisms, and structure*, John Wiley & Sons, 2007.
40. S. Martinez, I. Stern, *Applied surface science* 199 (2002) 83-89.
41. R.T.Vashi, V.A.Champaneri, *Indian J.Chem.Technol.* 180 (1997).
42. A.K. Mohamed, H.A. Mostafa, G.Y. El-Awady, A.S. Fouda, *Port. Electrochim. Acta* 18 (2000) 99.
43. M. El Achouri, S. Kertit, H.M. Goultaya, B. Nciri, Y. Bensouda, L. Perez, M.R. Infante, K. Elkacemi, *Progress in Organic Coatings* 43 (2001) 267-273.
44. F.B. Growcock, R.J. Jasinski, *Journal of the Electrochemical Society* 136 (1989) 2310-2314.
45. E. Machnikova, M. Puderova, M. Bazzaoui, N. Hackerman, *Surface & Coatings Technology* 202 (2008) 1543-1550.
46. C.H. Hsu, F. Mansfeld, *Corrosion* 57 (2001) 747-748.
47. R.W. Bosch, J. Hubrecht, W.F. Bogaerts, B.C. Syrett, *Corrosion* 57 (2001) 60-70.
48. Gamry Echem Analyst Manual (2003).
49. R.G. Kelly, J.R. Scully, D. Shoesmith, R.G. Buchheit, *Electrochemical techniques in corrosion science and engineering*, CRC Press, 2002.
50. K.F. Khaled, *Int. J. Electrochem. Sci* 3 (2008) 462-475.
51. K.F. Khaled, *Electrochimica Acta* 53 (2008) 3484-3492.
52. V.S. Sastri, E. Ghali, M. Elboujdaini, *Corrosion prevention and protection: practical solutions*, John Wiley & Sons Incorporated, 2007.
53. J. Cruz, T. Pandiyan, E. GarcÃ-a-Ochoa, *Journal of Electroanalytical Chemistry* 583 (2005) 8-16.
54. J. Fang, J. Li, *Journal of Molecular Structure: THEOCHEM* 593 (2002) 179-185.
55. N.K. Allam, *Applied surface science* 253 (2007) 4570-4577.
56. C. Lee, W. Yang, R.G. Parr, *Phys. Rev. A* 38 (1988) 3098.
57. R.M. Issa, M.K. Awad, F.M. Atlam, *Applied surface science* 255 (2008) 2433-2441.